Fatigue damage evaluation on austenitic stainless steel using nonlinear ultrasonic method

Chen Zhenhua[1, 4] Xu Guochen[1] Lu Wei[2] Chen Weibing[1] Lu Chao[1, 2]

(1. Key Laboratory of Nondestructive Testing of Ministry of Education, Nanchang Hangkong Universtiy, Nanchang 330063, China ; 2. Science and Technology on Power Beam Processes Laboratory, AVIC Manufacturing Technology Institute, Beijing 10024, 3. Gan Nan Normal University , Gan Zhou 341000, China ; 4. State Key Laboratory of Acoustics, Institute of Acoustics, Chinese Academy of Sciences, Beijing 100190, China)

Abstract: The closed crack and micro damage are liable to be underestimated in conventional (linear) ultrasonic nondestructive testing, which lead to unpredictable safety hazards. The objective of this work was to detect the fatigue damage in the stainless steel samples by use of nonlinear ultrasonic method. In the first, the macro cracks of fatigue specimens were measured by metallographic method. Secondly, the finite amplitude method of nonlinear ultrasonic testing was employed to evaluate the micro damages, and both the linear and the nonlinear characteristics of testing signals were investigated. Thirdly, the influences of excitation voltage on the finite amplitude method were discussed. The results indicate that the maximum value of the relative nonlinearity parameter is sensitive to the closed cracks and micro damages which are unable to be detected by the amplitude of linear ultrasonic testing. Higher excitation voltage is beneficial for exciting the nonlinear response of closed crack, which can be used to evaluate the degree of fatigue damage.

Key words: closed crack; micro-damage; relative nonlinearity parameter; stainless steel; metallographic method.

1. Introduction

The austenitic stainless structural components are widely employed in many engineering machines and infrastructures such as nuclear power plants, chemical industry and aerospace field, in terms of excellent corrosion resistance, economy, and mechanical properties [1, 2]. However, the more common application of stainless steel has been limited partly in dynamic load conditions due to a lack of understanding of performance and failure modes. Ultrasonic technology plays a vital role in material defect assessment, due to that the propagation characteristics of the ultrasonic wave can directly reflect the intrinsic property of the material in a nondestructive way [3, 4]. The nondestructive testing of austenitic stainless component can help us ensure the engineering material's safety and in-service integrity of the damage state. The traditional ultrasonic techniques are based on linear theory, what is the concern that the defects change the amplitude of the output signal with the same frequency of input signals. However, many researchers [5–7] have found that the traditional linear ultrasonic techniques are only sensitive to those gross defects and open crack. The sensitivity of linear ultrasonic techniques on the micro-void nucleation and microstructural variation occurred in the early stages confirmed to be relatively low.

The nonlinear ultrasonic technique has now been regarded as a powerful instrument to characterize the microstructural damages at an early stage [8–10]. The nonlinear ultrasonic technique is that the existence of the defects and discontinuities in the material could affect the amplitude of the output signal of the ultrasonic wave and change its frequency differing from that of the input signal [11]. When a sinusoidal ultrasonic wave of a single frequency with sufficient strength is introduced into an anharmonicity solid, the fundamental wave will be distorted by the nonlinear elastic response. As a result, the higher harmonic waves are generated in the transmitted wave, since the magnitude of harmonic waves depends on medium properties. Thus, the degradation of elastic property can be monitored by evaluating the higher harmonic wave's generated magnitude in the transmitted wave. Considering that a stainless steel component's service life mainly depends on the early damage stage such as void initiation and growth instead of the crack connection and propagation at the later stage, the void initiation and earlier damage should be detected as soon as possible. Hanying Mao[12] evaluated the gear's fatigue damage using the nonlinear ultrasonic method; second and third-order relative nonlinearity parameters are applied to estimate fatigue damage. Guo Shang Shui et al. [13] employed the acoustic nonlinearity parameter (ANP) based on the fundamental and second harmonics to characterize the adhesive joints' fatigue damage. Wenkai Li et al. [14] verified that the ultrasonic nonlinear parameter exhibits more significant sensitivity to fatigue damage like crack initiation and crack propagation. Shen, Y. et al. [15] investigated the nonlinear guided waves for fatigue crack detection and evaluation, and the Saturation effects and amplitude effects of nonlinear responses are also discussed.

In this work, the nonlinear ultrasonic technique was applied to evaluate the fatigue damage which cannot be detected by conventional ultrasonic testing. The excitation voltage influences on the nonlinearity parameter were also investigated for enhancing the testing capabilities. This paper is organized into the following parts: section 2 introduces the specimen preparation and metallographic measurement; section 3 discusses the nonlinear testing, and the nonlinear and linear characteristics are investigated; and the conclusions of this study are presented in section 4. The results demonstrate that the nonlinear ultrasonic testing can be used for evaluating the degree of the fatigue damage, and the higher excitation voltage is beneficial for exciting nonlinear responses.

2. Specimens with different fatigue cracks

The material used in this study is the AISI 304 austenitic stainless steel with following chemical composition given in Table 1.

Table 1 Chemical composition of 304 austenitic stainless steel (wt.%).

Element	C	Cr	Ni	Mn	Si	P	S	Fe
Content	0.068	18.2	8.59	1.24	0.408	0.070	0.003	Bal.

The fatigue specimens of austenitic stainless steel were manufactured according to the ASTM standard ASTM E468-1990 (2004). The low-frequency fatigue tests were performed on the MTS-C45 tensile testing machine. The strain-controlled fatigue provided a uniform accumulation of damage and limited deformation of the specimens, thus performing better than the stress-controlled fatigue. The *R* stress ratio and frequency of the fatigue examination were respective set to 0.1 and 10 Hz. The static examination results indicated that 0.2 mm is reasonable oscillation amplitudes (peak-to-peak) for stainless steel specimens [16]. Figure 1 shows the schematic of the fatigue specimen and the metallographic images of the fatigue cracks. Figure 1(a) shows the specimen's geometry is 131 x 30 x 30 mm, and an initial notch of 7 mm depth is introduced to obtain stress concentration. The fatigue loads of 332, 166, 83, and 50 Kilo-cycles were applied to the four specimens to produce the fatigue specimens with different damage degrees. The specimens with fatigue damages were cut along the white dashed frames (see Figure 1(a)) into the small pieces of about 24mm (length) x 23 mm (width) x 30 mm (thickness) for ultrasonic nondestructive measurement. The metallographic experiments were carried out to measure the crack extension in the specimen's surface. Figure 1(b) shows the maximum crack's length of the fatigue specimens of 331 Kilo-cycles, 166 Kilo-cycles, 83 Kilo-cycles, and 50 Kilo-cycles measured by the metallography is respective 4.39 mm, 5.26 mm, 9.27 mm and 9.15 mm. Besides, the angle between the crack and the detection surface β can also be measured. In the research, both ultrasonic linear and nonlinear techniques were carried out to evaluate the cracks' evolution in the fatigue specimens. Then evaluation results are compared with each other.

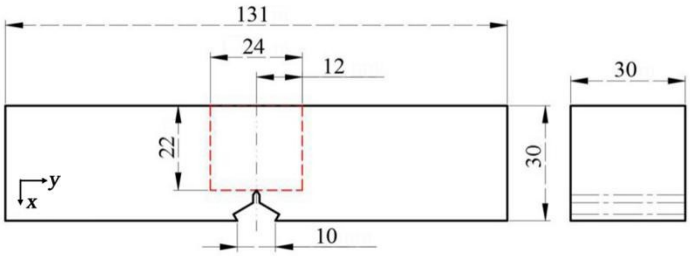

(a) Schematic of the fatigue specimen

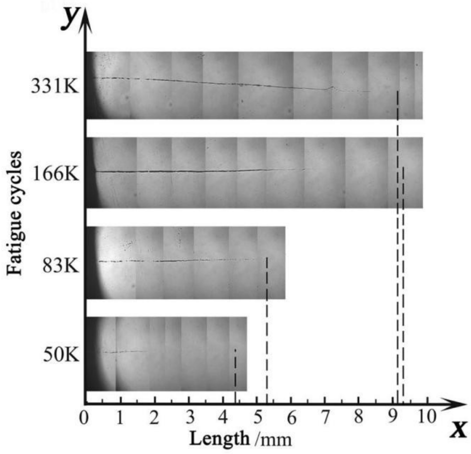

(b) Metallographic photos

Fig. 1 Testing specimen and it's metallographic photos

The macro-crack's length and direction β angle measured by the metallographic measurement are shown in Table 1. The β angle refers the angle between the crack's extension direction and specimen's surface. The crack's length in 50 K, 83 K, 166 K, 336 K fatigue specimen is respective 4.4 mm, 5.3 mm, 9.3 mm and 9.2 mm, which increases with the fatigue cycles. Moreover, the crack's width of 336 K fatigue specimen is bigger than that of 166 K fatigue specimen, which means the nonlinear ultrasonic response of 336 K fatigue specimen may be more difficult to be excited than that of 166 K specimen. Moreover, the β angle in 50 K, 83 K, 166 K, 336 K fatigue specimen is respective 2°、5°、7°、10°.

Table 2 Measurement results of metallographic photos

Fatigue cycles	Metallographic measurement	
	The maximum length (mm)	The Maximum β angle
336 K	9.2	10°

166 K	9.3	7°
83 K	5.3	5°
50 K	4.4	2°

3. The nonlinear ultrasonic measurement

3.1 Experimental apparatus and measurement

The commonly used nonlinear ultrasonic testing method is termed as the finite amplitude method, which excites the nonlinear ultrasonic response of defect and damage by enhancing the excitation voltage and wave's amplitude. The relative nonlinearity parameter r used for evaluating closed crack can be defined in as A_2/ A_1^2, where A_1 and A_2 is the voltage amplitude of the fundamental and second harmonic wave, respectively [19~21]. The center frequency of the second harmonic is twice the fundamental. Figure 2 shows the schematic diagram of the experimental setup. The testing system consists of two attenuators, several filter banks and one dual-channel digital oscilloscope. One transducer acted as a transmitter sending pulses across the specimen, collected by the other transducer as a receiver. The input signals of 2.5 MHz sinusoidal waves were generated from a high-voltage signal generator (RAM-5000). Higher voltage was transferred into a transmitter through a 50-ohm load, matching the generator and the transmitter's impedance. A high power gated amplifier produced the excitation voltage launched on the transmitter, and the attenuator was used for controlling the voltage amplitude. Moreover, low pass filtering was adopted to avoid higher frequency interference. The second harmonic with 5 MHz transmitted by the specimen containing the harmonic component was extracted from the receiver on the other side of the specimen. The received signal was sent to a 5 MHz band-pass filter, followed by the input into channel 2. The received fundamental signal with 2.5 MHz was attenuated, which was then input into channel 2. The computer can control the testing system; meanwhile, the test signals needed to be output on the oscilloscope. Since the coupling state between the probe and the specimen influences the extraction of nonlinear response significantly, the fixing device for coupling the transducers and the specimen were specially designed. The fixing device comprises a damping platform, a pressure screw assembly and a pressure sensor, as shown in Figure 2(b). The damping platform was used to reduce the interferences of external vibration. The pressure screw in the pressure screw assembly can be rotated to produce a suitable coupling pressure monitored by the pressure sensor. The secondary harmonic amplitude of the intact material measured by a non-interfering system is proportional to the fundamental amplitude square. The secondary wave and fundamental wave amplitudes in an intact specimen were measured under the exciting voltage from 175V to 420 V to confirm the detection system's anti-interference. The relationship between the square of the fundamental amplitude and the second harmonic amplitude under different excited voltages are shown in Figure 2c. The linear fitting is carried out for the measured values, and the 0.97 of Goodness of Fit indicated an excellent linear relationship. Thus, the test system, which is rarely affected by non-material nonlinearities, can extract the nonlinear ultrasonic response of microdamage in the fatigue specimen.

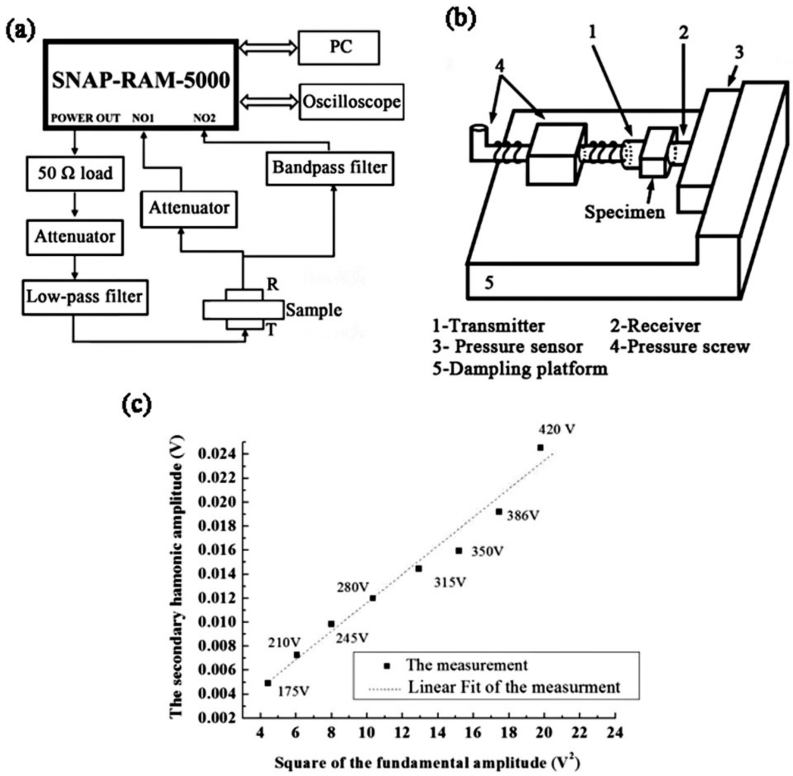

Fig. 2 Schematic diagram of the experiment setup. (a) Schematic diagram of the testing system, (b) Fix device, (c) The system testing.

Figure 3 shows the schematics of nonlinear ultrasonic testing. The 2.5 MHz transmitter and 5 MHz receiver with 12 mm diameter crystal were kept on the same axis to avoid energy loss. The transducers were arranged at a distance of 15 mm from the crack's initiation. The effective nonlinear ultrasonic response can only be excited from one defect or damage covered by the main sound beam, due to the mandatory factor of higher wave amplitude for the nonlinear ultrasonic response. The length of near sound filed *N* can be defined as follows:

$$N = \frac{D_s^2 - \lambda}{4\lambda} \tag{1}$$

Where: D_s^2 is the diameter of transducer's crystal, λ is wave length.

According to Eq. (1), the *N* of transmitting wave is 15 mm, and the length of the non-diffraction zone of transmitting sound field in the specimen is 1.64*N* which equals to 24.6 mm. The dotted line in figure 5 denotes the range of the main sound beam. The diameter of the main sound beam in the specimen equals to the crystal diameter (12 mm). Considering the length of the longest crack is 9.3 mm, and the β angle is 7°, the edge of the main ultrasonic beam almost cannot intersects with the end of the longest macro-crack (solid line), as shown in figure 5. Moreover, the main ultrasonic beam cannot cover the shorter macro-crack in the 50 Kilo and 83 Kilo-cycles' fatigue specimens.

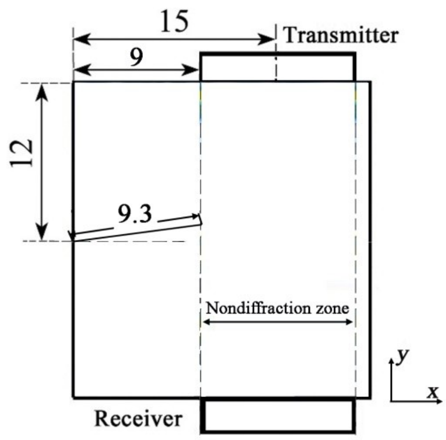

Fig. 3 The test schematics of nonlinear ultrasonic testing (mm)

4.2 The relative nonlinearity parameter varied with the crack extension

The pulse width of the excitation signal must be shorter than the travel time of ultrasound through the specimen to reduce the disturbance from equipment and random noise. Repeat examinations showed that an excitation signal of 2.5 MHz single-frequency sine pulse, 11 cycles, and 4.4 μs pulse width were suitable for the testing. Figure 6 shows the testing signals, and its frequency spectra of different fatigue cycles' specimen under the excitation voltage of 385 V. The testing signals exhibit the same width of about 4.75 μs. The amplitude A_1 at the fundamental frequency of 2.55 MHz and the amplitude A_2 at the second-harmonic frequency of 5.0 MHz are displayed in the frequency spectra, which are used to determine the relative nonlinearity parameter. The spectrum in figure 6 also demonstrates the stable amplitude of fundamental frequency, but the amplitudes of secondary harmonic increase with the fatigue cycles.

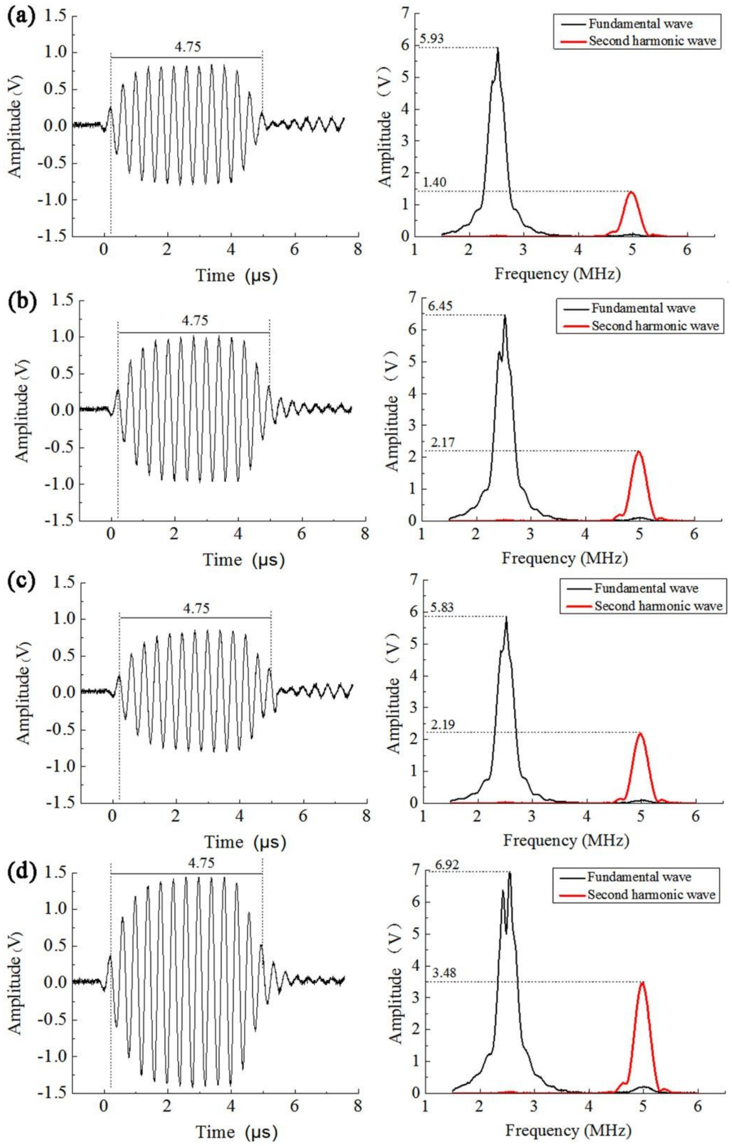

Fig. 4 The testing signals and its frequency spectra of fatigue specimens of different fatigue cycles. (a) 50 kilo-cycles, (b) 83 kilo-cycles, (c) 166 kilo-cycles, (d) 331 kilo-cycles.

4.3 Results and discussion

The excitation voltage plays a vital role in the finite-amplitude method. The nonlinear and the linear characteristics were extracted as the excitation voltage increases from 245 V to 420 V with an interval of 35 V. The fundamental amplitudes of each fatigue specimens under different excitation voltage are investigated. Figure 5(a) shows that the amplitude of fundamental wave A_1 increases with the excitation voltage. However, there is no monotonic relationship between the maximum fundamental amplitudes and fatigue cycles, as shown in figure 5(b). The fundamental amplitude based on the linear ultrasonic technique cannot be used for evaluating the fatigue damages, because the macro cracks are not covered by the main sound beam under the condition of this transducer's distribution.

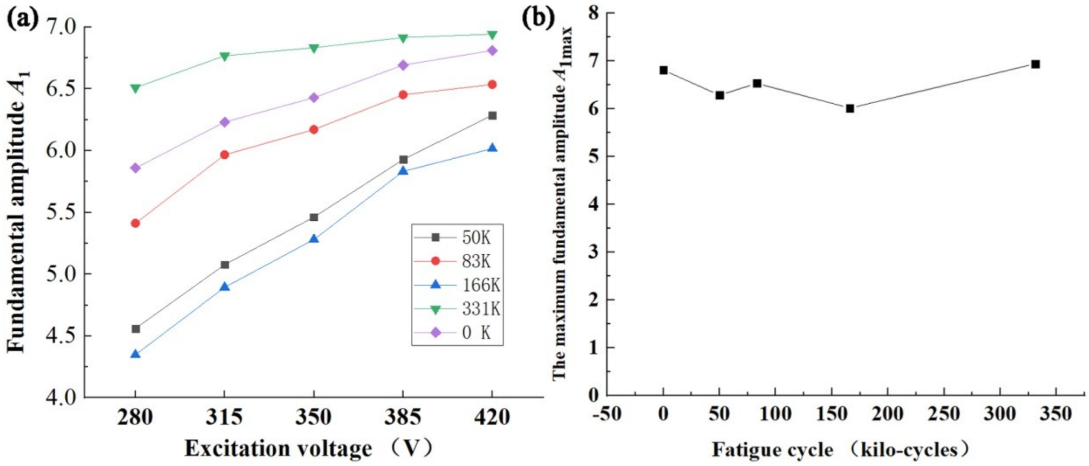

Fig. 5 The fundamental amplitudes of different fatigue specimen vary with the excitation voltage. (a) The fundamental amplitudes A_1 varied with the excitation voltage, (b) The A_{1max} varied with the fatigue cycles.

Figure 6(a) shows the r increases with the excitation voltage; thus, the higher excitation voltage is liable to excite the nonlinear ultrasonic response. The relative nonlinearity parameter r can keep constant with the increases of excitation voltage when there is no damage in the metal specimen, called the intrinsic nonlinearity, as shown in Figure 4c. However, the r of the crack called contact nonlinearity increases with the excitation voltage. The reasons are as follows:

(1) The contact nonlinearity is much more significant than the intrinsic nonlinearity.

(2) The wider crack needs a higher excited voltage to excite the opening and closing behavior (nonlinear ultrasonic response).

(3) Due to the crack's gap gradually decreasing from the initial opening to the end of the tip, the crack's length that contributes to nonlinear ultrasonic response increases with the increase of excitation voltage.

The metallographic measurement shows that the macro crack's length of 166 Kilo-cycles fatigue specimen (9.27 mm) is a little longer than that of 331 Kilo-cycles fatigue specimen. Nevertheless, the crack's gap of 331 Kilo-cycles fatigue specimen is wider after the crack extends to 6 mm. That is to say the increase in fatigue cycles makes the macro crack's gap wider. The excitation voltage required for exciting nonlinear ultrasonic response increases as the crack's gap becomes wider. The relative nonlinearity parameter r of the 166 Kilo cycles' specimen is higher than that of the 331 cycles' specimen within the excitation voltage of 280 V and 350 V, due to the nonlinear ultrasonic response of wider crack in the 331 Kilo cycles' specimen cannot be excited by lower excitation voltage. However, the nonlinear response of the wider crack in the specimen of 331 Kilo cycles is also excited when the voltage is further increased to 385 V, resulting in the highest relative nonlinearity parameter. Thus, the increased voltage contributes to stimulating the nonlinear ultrasonic response of wider crack, which could evaluate the fatigue damage more accurately. Fig. 6b shows that the maximum relative nonlinearity parameter r_{max} extracted from the highest voltage increases with the increased number of fatigue cycles; the r_{max} can be employed to evaluate the damage's degree. In particular, the growth rate in the range of 0 - 83 Kilo cycles is significantly higher than that in the range of 166 - 331 Kilo cycles, indicating that the r-value is more sensitive to the production of cracks and the growth of micro-cracks.

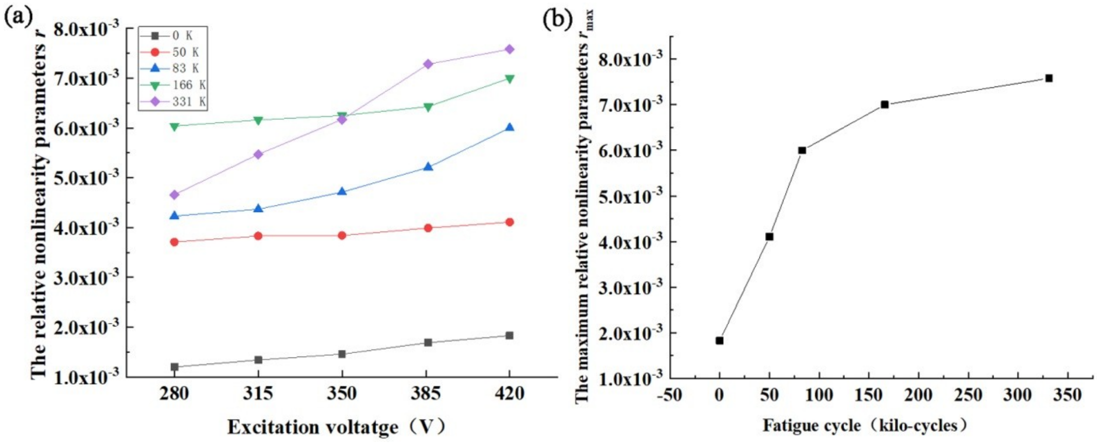

Fig. 6 The relative nonlinearity parameters of different fatigue specimen vary with the excitation voltage. (a) The relative nonlinearity parameters r varied with the excitation voltage, (b) The r_{max} varied with the fatigue cycles.

5. Conclusion

The linear and nonlinear ultrasonic techniques were employed to characterize the fatigue crack and damage of stainless steel. Firstly, the ultrasonic phased array method was adopted for the B scan imaging. The yellow-blue boundary is regarded as the crack's edge in the B scan image for measuring the crack's length. The testing accuracy is influenced by focus size, crack orientation β and crack closure degree, leading to the significant differences between the examination results and metallographic measurement. The accuracy can be improved by increasing the probe’s frequency to reduce the focus size. However, the crack size error will be inevitable due to the unpredictable crack closure and orientation during phased array testing. Secondly, the finite-amplitude method of nonlinear ultrasonic technology was adopted to evaluate the micro-damage, and the testing system with excellent anti-interference was obtained. The experimental results show that the higher excitation voltage is beneficial to excite nonlinear response of fatigue crack. The maximum relative nonlinearity parameter of each specimen increases monotonically with the degree of fatigue damage. Therefore, the maximum relative nonlinearity parameter can characterize the micro-damage, which is more sensitive to test crack initiation and micro-crack extension. In summary, the combination of nonlinear and linear ultrasonic technologies should be used to measure the crack's length and the damage degree. The macro crack length and the micro-damage degree can be measured by the linear and nonlinear methods, respectively.

Acknowledgments

The work presented in this paper was performed within the scope of the research project No. 11664027 and project No. SKLA201811 financed by National Natural Science Foundation of China and State key laboratory of acoustics of China, respectively. The third author would like to acknowledge his support from the research Project No. 11374134 financed by the National Natural Science Foundation of China.

Reference

[1] N. Baddoo, P. Francis, Development of design rules in the AISC design guide for structural stainless steel. Steel Constr. 2015, 83(83): 200-208.

[2] F. Yin, L. Yang, M. Wang, et al. Study on ultra-low cycle fatigue behavior of austenitic stainless steel. Thin-Walled Structures, 2019, 143: 1-11.

[3] Peng W , Zhang Y , Qiu B , et al. A Brief Review of the Application and Problems in Ultrasonic Fatigue Testing[J]. Aasri Procedia, 2012, 2(Complete):127-133.

[4] Maria V. Felice, Zheng Fan. Sizing of flaws using ultrasonic bulk wave testing: A review. Ultrasonic, 2018, 88: 26-42.

[5] Walker SV, Kim JY, Qu J, et al. Fatigue damage evaluation in A36 steel using nonlinear Rayleigh surface waves. NDT & E Int, 2012, 48(2):10-5.

[6] W. Li, Y. Cho, J. D. Achenbach. Assessment of heat treated inconel X-750 alloy by nonlinear ultrasonics. Exp. Mech. 2013, 53: 775-781.

[7] Weibin Li, Younho Cho. Combination of nonlinear ultrasonics and guided wave tomography for imaging the micro-defects. Ultrasonics, 2016, 65: 87-95.

[8] Hong M, Su Z, Wang Q, et al. Modeling nonlinearities of ultrasonic waves for fatigue damage characterization : theory, simulation, and experimental validation[J]. Ultrasonics, 2013, 54(3):770-778.

[9] Kim Y , Lim H J , Sohn H . Nonlinear ultrasonic modulation based failure warning for aluminum plates subject to fatigue loading[J]. International Journal of Fatigue, 2018, 114: 130-137.

[10] XiaoWang, Xue Wang, Xiao-guangNiu, De-ming Xiao, Xian-long, Hu. Application of nonlinear ultrasonic technique to characterize the creep damage in ASME T92 steel welded joints. NDT&E International. 2018, 98: 8-16.

[11] Jhang K Y. Nonlinear ultrasonic techniques for nondestructive assessment of micro damage in material: a review. Int J Precision Eng Manuf. 2009, 10 (1): 123-35.

[12] Hanying Mao, Yuhua Zhang, Hanling Mao, et al. The fatigue damage evaluation of gear in sugarcane presser using higher order ultrasonic nonlinear coefficients. Results in Physics. 2018, 10: 601-606.

[13] Guoshuang Shui, Yue-sheng Wang, Peng Huang, Jianmin Qu. Nonlinear ultrasonic evaluation of the fatigue damage of adhesive joints. NDT&E International, 2015, 70: 9-15.

[14] Wenkai Li, Haitao Cui, Weidong Wen, Xuming Su. In situ nonlinear ultrasonic for very high cycle fatigue damage characterization of a cast aluminum alloy. Materials Science & Engineering A. 2015, 248-254.

[15] Shen, Y, Wang, J, Wu, X. "Nonlinear features of guided waves scattering from rivet hole nucleated fatigue cracks considering the rough contact surface conditions", Smart Materials and Structures, 2018, 27(10): 1-15.

[16] Andrei Zagrai, Dimitri Donskoy, Alexander Chudnovsky, Edward Golovin. Micro- and Macroscale Damage Detection Using the Nonlinear Acoustic Vibro-Modulation Technique. Research in Nondestructive Evaluation, 2008, 19(2): 104-128.

[17] Lingyu Yu, Zhenhua Tian. Guided wave phased array beam forming and imaging in composite plates. Ultrasonics, 2016, 68: 43-53.

[18] GAO M, WANG C, CAI F, et al. Research on Ultrasonic Real-time Multiple Focusing In the Three Dimensional Space [J]. Technical Acoustics, 2016, 35: 424-426.

[19] Bermes C , Kim J Y , Qu J , et al. Experimental characterization of material nonlinearity using Lamb waves[J]. Applied Physics Letters, 2007, 90(2): 2067-2073.

[20] Masurkar F., Tse P W., Yelve N. Investigating the critical aspects of evaluating the material nonlinearity in metal plates using Lamb waves: Theoretical and numerical approach [J]. Applied Acoustics, 2018, 140(NOV.): 301-314.

[21] Kim J , Song D G , Jhang K Y . A method to estimate the absolute ultrasonic nonlinearity parameter from relative measurements[J]. Ultrasonics, 2017, 77: 197-202.

Author Contribution Statement:

All persons who meet authorship criteria are listed as authors, and all authors certify that they have participated sufficiently in the work to take public responsibility for the content, including participation in the concept, design, analysis, writing, or revision of the manuscript. The contributions corresponding to each author are listed below:

(1) Chen Zhenhua: Conception and design of study, analysis and/or interpretation of data, Drafting the manuscript;

(2) Xu Guochen: acquisition of data, analysis and/or interpretation of data;

(3) Lu Wei: acquisition of data, analysis and/or interpretation of data;

(4) Chen Weibing: acquisition of data, analysis and/or interpretation of data;

(5) Lu Chao: revising the manuscript critically for important intellectual content.